

Nitrogen defects and ferromagnetism in Cr-doped dilute magnetic semiconductor AlN from first principles

Li-Jie Shi,^{*} Li-Fang Zhu, Yong-Hong Zhao, and Bang-Gui Liu[†]

Institute of Physics, Chinese Academy of Sciences, Beijing 100190, China

and Beijing National Laboratory for Condensed Matter Physics, Beijing 100190, China

(Received 27 July 2008; revised manuscript received 20 October 2008; published 13 November 2008)

High Curie temperature of 900 K has been reported in Cr-doped AlN diluted magnetic semiconductors prepared by various methods, which is exciting for spintronic applications. It is believed that N defects play important roles in achieving the high-temperature ferromagnetism in good samples. Motivated by these experimental advances, we use a full-potential density-functional-theory method and supercell approach to investigate N defects and their effects on ferromagnetism of (Al,Cr)N with N vacancies (V_N). We investigate the structural and electronic properties of V_N , single Cr atom, Cr-Cr atom pairs, Cr- V_N pairs, and so on. In each case, the most stable structure is obtained by comparing different atomic configurations optimized in terms of the total energy and the force on every atom, and then it is used to calculate the defect formation energy and study the electronic structures. Our total-energy calculations show that the nearest substitutional Cr-Cr pair with the two spins in parallel is the most favorable and the nearest Cr- V_N pair makes a stable complex. Our formation energies indicate that V_N regions can be formed spontaneously under N-poor condition because the minimal V_N formation energy equals -0.23 eV or Cr-doped regions with high enough concentrations can be formed under N-rich condition because the Cr formation energy equals 0.04 eV, and hence real Cr-doped AlN samples are formed by forming some Cr-doped regions and separated V_N regions and through subsequent atomic relaxation during annealing. Both of the single Cr atom and the N vacancy create filled electronic states in the semiconductor gap of AlN. N vacancies enhance the ferromagnetism by adding μ_B to the Cr moment each but reduce the ferromagnetic exchange constants between the spins in the nearest Cr-Cr pairs. These calculated results are in agreement with experimental observations and facts of real Cr-doped AlN samples and their synthesis. Our first-principles results are useful to elucidate the mechanism for the ferromagnetism and to explore high-performance Cr-doped AlN diluted magnetic semiconductors.

DOI: [10.1103/PhysRevB.78.195206](https://doi.org/10.1103/PhysRevB.78.195206)

PACS number(s): 75.90.+w, 71.20.-b, 75.50.-y, 75.75.+a

I. INTRODUCTION

The diluted magnetic semiconductor (DMS) is of great interest because it has merits of both semiconductor and spin magnetism. Especially the possibility of high-temperature ferromagnetism in DMSs has inspired scientists from all over the world to explore new promising DMS materials and study their physical properties for spintronic applications.^{1,2} (Ga,Mn)As has been studied substantially because of its close relation with important GaAs semiconductor, and its ferromagnetism is believed to be induced by hole carriers.^{3,4} Generally speaking, it is believed that at least 500 K as Curie temperature is necessary for real spintronic devices to work at room temperature.⁵ Curie temperature higher than 500 K is achieved in various transition-metal doped oxides⁶⁻¹⁴ and nitrides.^{15,16} For Cr-doped AlN, or (Al,Cr)N, a high Curie temperature of 900 K has been reported by several groups.¹⁷⁻¹⁹ It is shown that the high-temperature ferromagnetism in (Al,Cr)N materials is intrinsic, not produced by secondary phases.¹⁶⁻²² Naturally, such high Curie temperatures make the materials promising for practical spintronic applications.¹ Although ferromagnetism of (Ga,Mn)As DMS materials is believed to be induced by their effective carriers,^{3,4} the high-temperature ferromagnetism of (Al,Cr)N materials must be caused by different mechanism because some single-phase (Al,Cr)N samples with high Curie temperatures are highly insulating^{21,22} (the same as pure AlN)²³ or in the regime of variable-range hopping conduction²⁴

[similar to (Ga,Cr)N].²⁵ The ferromagnetism should be attributed to pd hybridization of Cr d states and N p ones.²⁶⁻²⁸ On the other hand, defects and impurities are believed to play important roles in DMS materials of wide semiconductor gaps.^{14,21,22,29-33} Nitrogen pressure during synthesis is shown to affect the ferromagnetism in resultant samples.^{21,22,30} It appears that reduced N content enhances the ferromagnetism, being in contrast with first-principles-calculated trend of N vacancies in the case of GaN-based DMSs.³⁴ Therefore, it is highly desirable to investigate effect of N content on the high-temperature ferromagnetism in (Al,Cr)N materials, and in return its elucidation is helpful to obtain deeper insight into the essential mechanism of the high-temperature ferromagnetism.

In this paper we use a full-potential density-functional-theory (DFT) method and $3 \times 3 \times 2$ supercell approach to investigate N defects and their effects on ferromagnetism of (Al,Cr)N with N vacancies (V_N), namely, $\text{Cr}_x\text{Al}_{1-x}\text{N}_{1-y}$. We obtain the most stable structures of $\text{Al}_{36}\text{N}_{35}$ (one V_N in the supercell), $\text{CrAl}_{35}\text{N}_{36}$ (one substitutional Cr in the supercell), $\text{CrAl}_{35}\text{N}_{35}$ (one V_N and one substitutional Cr atom in the supercell), $\text{Cr}_2\text{Al}_{34}\text{N}_{36}$ (two substitutional Cr atoms in the supercell), and so on by comparing their different atomic configurations optimized in terms of the total energy and the force on every atom, and thereby calculate their defect formation energies. Then we investigate the structural and electronic properties of V_N , single Cr atom, Cr-Cr pairs, and Cr- V_N pairs. Without N vacancy, the nearest substitutional

Cr-Cr pair with its moments orienting in parallel is the most favorable in total energy. The nearest pair of an N vacancy and a single Cr atom forms a stable complex of Cr^- and V_{N}^+ . Our calculated formation energies indicate that V_{N} regions can be formed spontaneously under N-poor condition or high enough Cr concentrations can be formed under N-rich condition, and hence real $\text{Al}_{1-x}\text{Cr}_x\text{N}_{1-y}$ samples are formed by forming Cr-doped regions and some separated V_{N} regions and through subsequent atomic relaxation during annealing. The doped Cr atom and the N vacancy create filled electronic states in the semiconductor gap of AlN. V_{N} enhances the ferromagnetism by giving one electron to a Cr ion to add μ_B to the Cr moment, which is in agreement with experimental observation that low N pressure during synthesis is helpful to obtain better ferromagnetic $\text{Al}_{1-x}\text{Cr}_x\text{N}_{1-y}$ samples.^{22,30} On the other hand, V_{N} reduces the ferromagnetic exchange constants between the spins in the nearest Cr-Cr pairs, which is consistent with experimental fact that too many N vacancies are harmful to the ferromagnetism when the synthesis temperature is high enough to allow doped Cr atoms to diffuse. These first-principles results are useful to explore high-performance (Al,Cr)N DMS samples and to understand the high-temperature ferromagnetism.

The remaining part of this paper is organized as follows. We shall present our computational method and parameters in Sec. II. In Sec. III, we shall present our main results of optimized magnetic structures (through geometric and internal atomic position optimizations) and defect formation energies. In Sec. IV, we shall present main electronic structures, including energy bands and electron-density distributions. In Sec. V, we shall discuss the ferromagnetism correlated with N defects in real samples. Finally, we shall give our main conclusion in Sec. VI.

II. COMPUTATIONAL METHOD AND PARAMETERS

We use a first-principles method and supercell approach to study wurtzite AlN with doped Cr atoms and N defects (including nitrogen vacancies and nitrogen interstitials). We use a $3 \times 3 \times 2$ supercell as shown in Fig. 1 and substitute a Cr atom for an Al atom to model Cr doping concentration of 2.78% realized in molecular-beam epitaxy (MBE) samples.^{16,18,19,21} This supercell is not very large to simulate real experimental conditions, but it is large enough to model the representative concentrations of both doped Cr and V_{N} and main properties of Cr-Cr and Cr- V_{N} interactions, especially considering that our calculations are done with full-potential linear augmented plane-wave (FLAPW) method within the DFT.³⁵ Using such supercell is also supported by the following calculated results that the total energy of both $\text{Cr}_{\text{Al}}\text{-Cr}_{\text{Al}}$ and $\text{Cr}_{\text{Al}}\text{-}V_{\text{N}}$ pairs substantially increases with increasing the $\text{Cr}_{\text{Al}}\text{-Cr}_{\text{Al}}$ and $\text{Cr}_{\text{Al}}\text{-}V_{\text{N}}$ distances, respectively. The supercell consists of one Cr atom, 35 Al atoms, and 36 N atoms and its space group is No. 156. Such a supercell for the pure AlN consists of 36 Al and 36 N atoms. The second Cr atom is introduced by substituting for one of Al atoms in the supercell. For example, Cr1 is made by substituting a Cr atom for the Al atom labeled as Al1 in Fig. 1. A nitrogen vacancy V_{N} is created by removing one N atom. For examples $V_{\text{N}1}$ (or

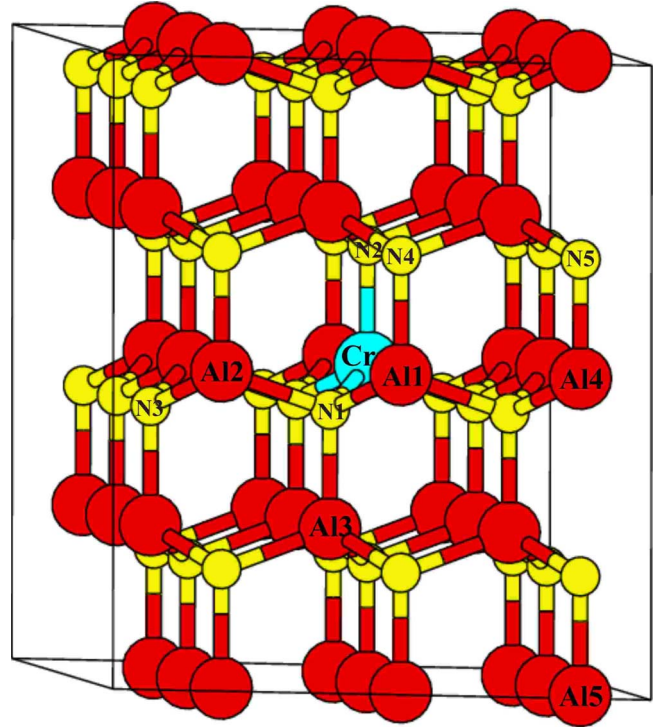


FIG. 1. (Color online) Schematic structure of Cr-substituted $3 \times 3 \times 2$ wurtzite AlN supercell $\text{CrAl}_{35}\text{N}_{36}$. The centering largest (cyan or white) ball is the first Cr atom, the smallest (yellow or light gray) ones are N atoms, and the other (red or gray) ones are Al atoms. An N vacancy can be created by removing an N atom and the second substitutional Cr atom can be introduced by substituting a Cr for an Al atom. For example, $V_{\text{N}1}$ (or V_1) is made by removing N1, and Cr3 by substituting a Cr atom for Al3.

V_1) is made by removing the N atom labeled as N1. An interstitial N atom is introduced by adding an N atom in the supercell. We obtain an octahedral N interstitial N_{T} if adding an N atom at an octahedral site or obtain a tetrahedral N interstitial N_{T} if adding an N atom at a tetrahedral site. We optimize lattice constants to minimize the total energy and at the same time optimize internal atomic coordinates to make the force on every atom less than $0.04 \text{ eV}/\text{\AA}$. All the electronic structures and magnetic moments are calculated with equilibrium lattice constants.

All the presented results are calculated with the full-potential linear augmented plane-wave method within the density-functional theory,³⁵ as implemented in the package WIEN2K,³⁶ although we also use pseudopotential method to do some preliminary structural optimizations. The generalized gradient approximation (GGA) (Ref. 37) is used as the exchange-correlation potential for all our presented results, and some important cases are confirmed by local-density-approximate calculations.³⁸ Full relativistic calculations are done for core states and the scalar approximation is used for the others, with the spin-orbit coupling being neglected.³⁹ The radii of muffin-tin spheres R_{mt} are adjusted so as to achieve the best accuracy of self-consistent calculations. We use the parameter $R_{\text{mt}}K_{\text{max}}=8.0$ and make the sphere harmonic expansion up to $l_{\text{max}}=10$ in the spheres. The Brillouin-zone integrations are performed with the special k point

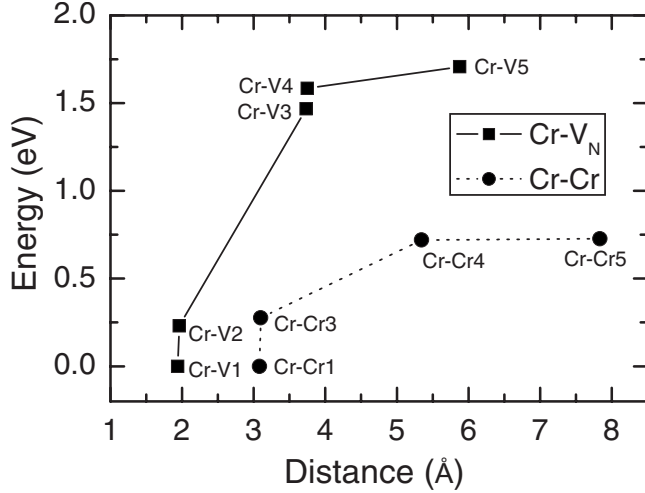


FIG. 2. Relative total energy of the Cr-doped AlN with N vacancies for different Cr- V_N distances (filled squares) and that of Cr-doped AlN for different Cr-Cr distances (filled circles). Here Cr-Cr n means the pair of the first Cr and the second Cr at the Al n site, and Cr- V_n the pair of the first Cr and the N vacancy at the N n site, as labeled in Fig. 1. The two smallest total energies, corresponding to the nearest Cr- V_N and Cr-Cr pairs, are set to zero.

method over a $5 \times 5 \times 3$ Monkhorst-Pack mesh. A convergence standard, $\int |\rho_n - \rho_{n-1}| dr < 0.00005$ (ρ_n and ρ_{n-1} are output and input charge densities, respectively), is used for all our self-consistent calculations.

III. OPTIMIZED STRUCTURES AND DEFECT FORMATION ENERGIES

We optimize fully the lattice structures and internal atomic positions for N vacancy ($\text{Al}_{36}\text{N}_{36} + V_N = \text{Al}_{36}\text{N}_{35}$), Cr-doped AlN ($\text{CrAl}_{35}\text{N}_{36}$), Cr atom plus N vacancy ($\text{CrAl}_{35}\text{N}_{36} + V_N = \text{CrAl}_{35}\text{N}_{35}$), Cr atom plus tetrahedral N interstitial ($\text{CrAl}_{35}\text{N}_{36} + N_T$), and Cr atom plus octahedral N interstitial ($\text{CrAl}_{35}\text{N}_{36} + N_O$). We can have various atomic configurations for pairs of Cr- V_N , Cr- N_T , and Cr- N_O with a given distance, and they correspond to different total energies. As for $\text{CrAl}_{35}\text{N}_{36} + V_N$, the total energy changes with the distance between Cr and V_N , and the lowest total energy is reached when Cr and V_N are the nearest neighbors Cr-V1 (connected with an approximately horizontal Cr-N bond). The next lowest total energy (0.23 eV) is reached by Cr-V2. For double Cr-doped system, the total energy depends on the Cr-Cr distance, and the lowest total energy is reached when the two Cr (Cr and Cr1) are in the same layer and connected with the same N (consistent with previous result⁴⁰). The next lowest total energy (0.28 eV) is reached by Cr-Cr3 and other equivalent Cr-Cr pairs. These trends are shown in Fig. 2.

Our systematic calculations show that a doped Cr atom contributes $3\mu_B$ to the total magnetic moment, and a neighboring N vacancy adds μ_B because its electron just below the Fermi level is transferred to the Cr d state. Actually, an isolated N vacancy, even without any Cr doping, has a moment of μ_B , but N vacancies are in paramagnetic order because intervacancy spin interaction is equivalent to zero within

TABLE I. The calculated equilibrium lattice constants (a/c), the relative volume change (δv) with respect to the pure AlN, the magnetic moment per magnetic atom (M), and the electronic density of states at the Fermi level (D_F). The pure AlN phase is presented for comparison.

Name	a/c (Å)	δv (%)	M (μ_B)	D_F
$\text{Al}_{36}\text{N}_{36} + V_N$	9.65/10.29	1.74	1.000	>0
$\text{CrAl}_{35}\text{N}_{36}$	9.59/10.26	0.21	3.000	>0
$\text{CrAl}_{35}\text{N}_{36} + V_{N1}$	9.58/10.22	-0.16	4.000	0
$\text{CrAl}_{35}\text{N}_{36} + N_{T1}$	9.66/10.26	1.28	2.000	0
$\text{CrAl}_{35}\text{N}_{36} + N_{O1}$	9.61/10.29	1.15	4.000	0
$\text{Al}_{36}\text{N}_{36}$	9.58/10.27	0.00	0.000	0

computational error. As for interstitial N atoms, a tetrahedral N carries a moment of $-\mu_B$ and an octahedral N has μ_B , but they are too high in total energy to exist in real samples. Two neighboring Cr atoms, such as Cr-Cr1 and Cr-Cr3, have $6\mu_B$ because their ferromagnetic couplings are favorable in energy. In fact, the ferromagnetic orientation is lower in total energy by 464 and 195 meV than the corresponding antiferromagnetic one for Cr-Cr1 and Cr-Cr3, respectively. The energy difference of 464 meV is decreased to 163 meV when one N vacancy is at the nearest site and is further reduced to 25 meV when two N vacancies are in the nearest neighborhood. This trend is consistent with effect of N vacancy on Mn-Mn spin-exchange constants.³⁴ The lattice constants, the relative volume changes, and the magnetic moments per supercell of the most stable configurations are summarized in Table I. The most stable is the N interstitial N_{T1} (N_{O1}), the nearest to the Cr atom, in $\text{CrAl}_{35}\text{N}_{36} + N_{T1}$ ($\text{CrAl}_{35}\text{N}_{36} + N_{O1}$) among all the tetrahedral (octahedral) N interstitials. The corresponding results for the pure AlN are also presented for comparison. The density of states (DOS) at the Fermi level D_F is zero in all the cases except for $\text{CrAl}_{35}\text{N}_{36}$ whose Fermi level is at the Cr d impurity bands and for $\text{Al}_{36}\text{N}_{36} + V_N$ whose Fermi level is at the N-vacancy-induced in-gap band.

We further calculate formation energy for all the cases. The formation energy of the supercell including n_{V_N} N vacancies and n_{Cr} substitutional Cr atoms is defined as^{41,42}

$$E_f(n_{V_N}, n_{Cr}) = E(n_{V_N}, n_{Cr}) - E(0, 0) + n_{V_N}\mu_N - n_{Cr}\mu_{Cr} + n_{Cr}\mu_{Al}, \quad (1)$$

where $E(n_{V_N}, n_{Cr})$ is the total energy of the supercell and ($\mu_N, \mu_{Cr}, \mu_{Al}$) are chemical potentials of N, Cr, and Al. Using $\mu_N^{\text{gas}}, \mu_{Al}^{\text{bulk}}$, and μ_{Cr}^{bulk} as the chemical potentials of N gas, Cr bulk, and Al bulk, we have $\mu_N = \mu_N^{\text{gas}} + \bar{\mu}_N$, $\mu_{Al} = \mu_{Al}^{\text{bulk}} + \bar{\mu}_{Al}$, and $\mu_{Cr} = \mu_{Cr}^{\text{bulk}} + \bar{\mu}_{Cr}$. The thermodynamical stability of AlN requires

$$\bar{\mu}_N + \bar{\mu}_{Al} = \bar{\mu}_{AlN}. \quad (2)$$

The fact that there is no spontaneous formation of CrN implies

TABLE II. The formation energies (ΔE) of a substitutional Cr atom and an N vacancy and their pairs in AlN. The +, 0, and - superscripts mean that the extra charge is equivalent to e , 0, and $-e$, where e is the absolute value of the electronic charge. The last row corresponds to the case where the distance between Cr and V_N is the longest within the $3 \times 3 \times 2$ supercell and the fourth row to the case where the distance is the shortest.

Name	ΔE (eV)
$\text{Al}_{36}\text{N}_{36} + V_{\text{N}1}$	-0.23
$\text{Al}_{36}\text{N}_{36} + V_{\text{N}}^+$	0.1 ^a
$\text{Cr}^0\text{Al}_{35}\text{N}_{36}$	0.04
$\text{Cr}^-\text{Al}_{35}\text{N}_{36} + V_{\text{N}1}^+$	0.77
$\text{Cr}^-\text{Al}_{35}\text{N}_{36} + V_{\text{N}5}^+$	2.47

^aReference 44.

$$\bar{\mu}_{\text{N}} + \bar{\mu}_{\text{Cr}} \leq \bar{\mu}_{\text{CrN}}. \quad (3)$$

We can express the minimal formation energy as

$$E_f^{\text{min}}(n_{V_{\text{N}}}, n_{\text{Cr}}) = E(n_{V_{\text{N}}}, n_{\text{Cr}}) - E(0, 0) + n_{V_{\text{N}}} \mu_{\text{N}}^{\text{gas}} - n_{\text{Cr}} (\mu_{\text{Cr}}^{\text{bulk}} - \mu_{\text{Al}}^{\text{bulk}}) + n_{V_{\text{N}}} \bar{\mu}_{\text{N}}^{\text{min}} - n_{\text{Cr}} (\bar{\mu}_{\text{Cr}}^{\text{max}} - \bar{\mu}_{\text{Al}}^{\text{min}}), \quad (4)$$

where the superscript max (min) means the maximum (minimum) of the chemical potential. The chemical potentials $\mu_{\text{N}}^{\text{gas}}$, $\mu_{\text{Al}}^{\text{bulk}}$, and $\mu_{\text{Cr}}^{\text{bulk}}$ can be calculated in terms of total energies of N gas, Al bulk, and Cr bulk. The maximal and minimal chemical potentials can be obtained in terms of equality (2) and inequality (3) and, therefore, the minimal formation energy can be calculated in terms of Eq. (4) as long as $\bar{\mu}_{\text{CrN}}$ and $\bar{\mu}_{\text{AlN}}$ are known.

Our calculated result is $\bar{\mu}_{\text{AlN}} = -3.33$ eV for AlN, and we use known data $\bar{\mu}_{\text{CrN}} = -1.30$ eV for CrN.⁴³ For a single neutral N vacancy in AlN under poor N condition, we have $n_{V_{\text{N}}} = 1$ and $n_{\text{Cr}} = 0$, and thus the formation energy is -0.23 eV, while the formation energy of a single N^+ vacancy is 0.1 eV.⁴⁴ For a neutral Cr atom under rich N condition, we have $n_{V_{\text{N}}} = 0$ and $n_{\text{Cr}} = 1$, and thus the formation energy is 0.04 eV. This small formation energy of 0.04 eV is reasonable and consistent with experimental high Cr doping concentrations.^{16,17,24,29,30} A previous unreasonably high formation energy of 3.01 eV (Ref. 45) is in contradiction with the experimental high Cr doping concentrations. Charged Cr atoms have much higher formation energies. For the nearest Cr- $V_{\text{N}1}$ pair, we have $n_{V_{\text{N}}} = 1$ and $n_{\text{Cr}} = 1$, and thus the formation energy is 0.77 eV, while more separated Cr- $V_{\text{N}5}$ pairs have higher formation energies. These results are summarized in Table II. Interstitial N atoms, both tetrahedral and octahedral, have very high total energies and formation energies, and therefore are not presented in Table II. This implies that either dilute N vacancies or dilute Cr atoms are easy to be realized in AlN because the interactions can be neglected in the dilute doping limit.

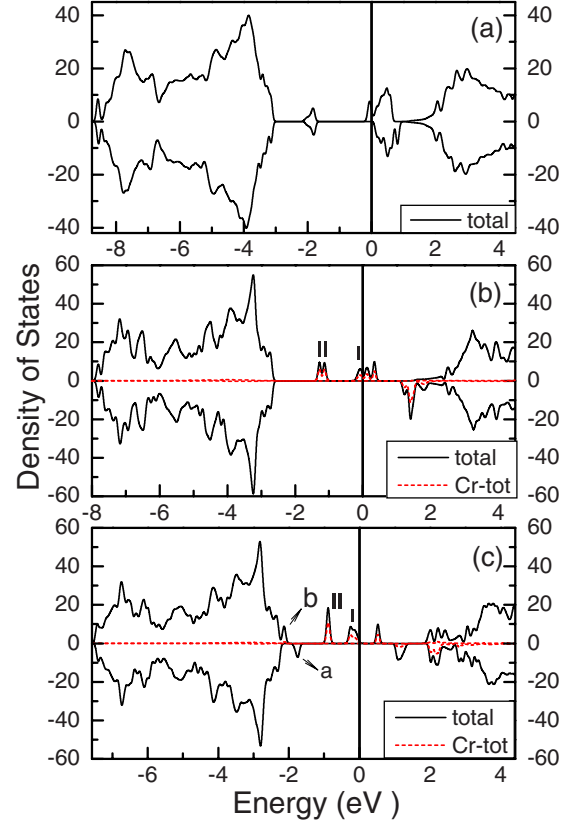


FIG. 3. (Color online) Spin-dependent total DOS (black solid lines) and Cr d partial DOS (red or gray dash lines) of (a) $\text{Al}_{36}\text{N}_{35}$ (including one V_{N}), (b) $\text{CrAl}_{35}\text{N}_{36}$ (including one Cr atom), and (c) $\text{CrAl}_{35}\text{N}_{35}$ (including one Cr+ $V_{\text{N}1}$ complex). The upper half for each panel is for majority-spin channel and the other for minority spin. For $\text{Al}_{36}\text{N}_{35}$, the filled part just below the Fermi level contains one electron, and thus one V_{N} contributes μ_B . For $\text{CrAl}_{35}\text{N}_{36}$, there is one electron in the small part I and two in the filled part of II, and hence the total moment is $3\mu_B$. For $\text{CrAl}_{35}\text{N}_{35}$, both I and II are filled with two electrons, and the total moment is $4\mu_B$. The small parts a and b, both filled with one electron, are due to V_{N} .

IV. ELECTRONIC STRUCTURES

We present spin-dependent DOS of $\text{Al}_{36}\text{N}_{35}$ (including one N vacancy in the supercell), $\text{CrAl}_{35}\text{N}_{36}$ (including one Cr substitutional at an Al site), and $\text{CrAl}_{35}\text{N}_{35}$ (including one Cr+ $V_{\text{N}1}$ complex) in Fig. 3. The valence bands for every spin channel are filled with 108 electrons for the AlN supercell, and in total we have 216 electrons in the valence bands. The absence of one N atom removes $3p$ electrons and reorganizes the band structures, as shown in Fig. 3(a). Now there are three electrons in the gap of AlN and the valence-band manifold is filled with 210 electrons, 105 for each spin channel. The N vacancy cannot donate electron to the conduction bands because the Fermi level is too low with respect to the conduction bands. This is different from the N vacancy of GaN.⁴⁶ Figure 3(b) shows the DOS of $\text{CrAl}_{35}\text{N}_{36}$. In this case we have 108 electrons in the valence-band manifold for each spin channel and the Cr d states are in the gap of AlN. The d states are split into a doublet (labeled as II) and a triplet (labeled as I). The former is filled with two electrons and the

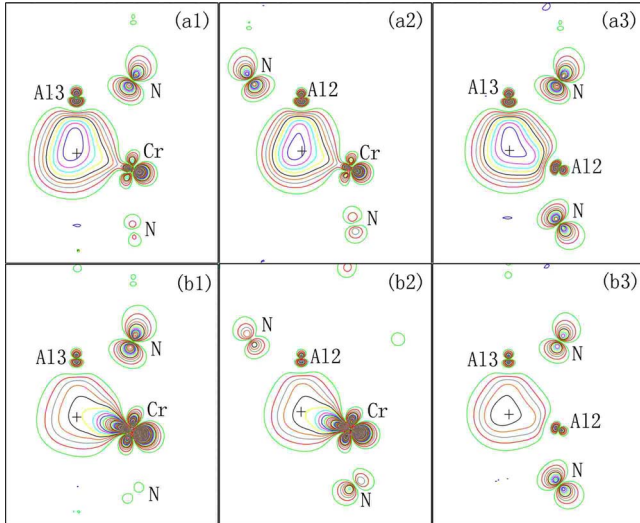


FIG. 4. (Color online) Electron-density distributions of the a and b bands of $\text{CrAl}_{35}\text{N}_{35}$ defined in panel (c) of Fig. 3. a1, a2, and a3 (b1, b2, and b3) show the electron-density distributions of the a (b) bands in the three planes defined by $\text{Cr}-V_{\text{N}1}-\text{Al}3$, $\text{Cr}-V_{\text{N}1}-\text{Al}2$, and $\text{Al}2-V_{\text{N}1}-\text{Al}3$, where Cr, Al1, Al2, and Al3 means the atoms labeled with the same signs in Fig. 1 and $V_{\text{N}1}$ is at the N1 site, labeled as +, connecting the Cr atom and three Al ones. The outmost (green or light gray) line represents $0.001e/\text{a.u.}^3$. The density contour increment is $0.001e/\text{a.u.}^3$.

latter by one. The Fermi level is in the bands of the triplet. Hence one Cr contributes $3\mu_B$ to the moment. In Fig. 3(c) we show the density of states of $\text{CrAl}_{35}\text{N}_{35}$. The interaction of the doped Cr and the N vacancy makes the filled singlet originating from the N vacancy move lower in energy and become two spin-split parts “a” and “b” and at the same time makes the Cr d triplet split into a doublet [also labeled as I in Fig. 3(c)] and a singlet. The valence-band manifold below part b consists of $105+105$ filled states. As a result, one Cr + V_{N} complex contributes $4\mu_B$ to the moment.

We present in Fig. 4 electron-density distribution of the N-vacancy-induced filled states, parts a and b indicated in Fig. 3(c), of $\text{CrAl}_{35}\text{N}_{35}$. The three planes are defined by three-site series: $\text{Cr}-V_{\text{N}}-\text{Al}3$, $\text{Cr}-V_{\text{N}}-\text{Al}2$, and $\text{Al}2-V_{\text{N}}-\text{Al}3$. Here Cr, Al1, Al2, and Al3 are the atoms labeled with the same signs in Fig. 1. It can be seen that the charge-density distribution at the N vacancy is about $0.014e/\text{a.u.}^3$, where e is the absolute value of the electronic charge. The total charge within the N vacancy is estimated to be approximately equivalent to $1.1e$. The remaining $0.9e$ charge of parts a and b is distributed at the nearest Cr site ($0.6e$) and N site ($0.3e$). This indicates that the N-vacancy state is substantially hybridized with the Cr d states and substantial charge is transferred to the vacancy from the neighboring Al (or Cr) atoms although there is no N atom at the site.

We present in Fig. 5 the Cr d electron-density distribution of $\text{CrAl}_{35}\text{N}_{36}$ and $\text{CrAl}_{35}\text{N}_{35}$. The three planes are the same as those in Fig. 4. For $\text{CrAl}_{35}\text{N}_{36}$, it is estimated approximately that 80% of the II charge is around the Cr atom, 70% of the I charge is around Cr, and the Cr electronic configuration is d^3 . For $\text{CrAl}_{35}\text{N}_{35}$, approximately 90% of the II charge is around the Cr atom and 85% of the I charge is

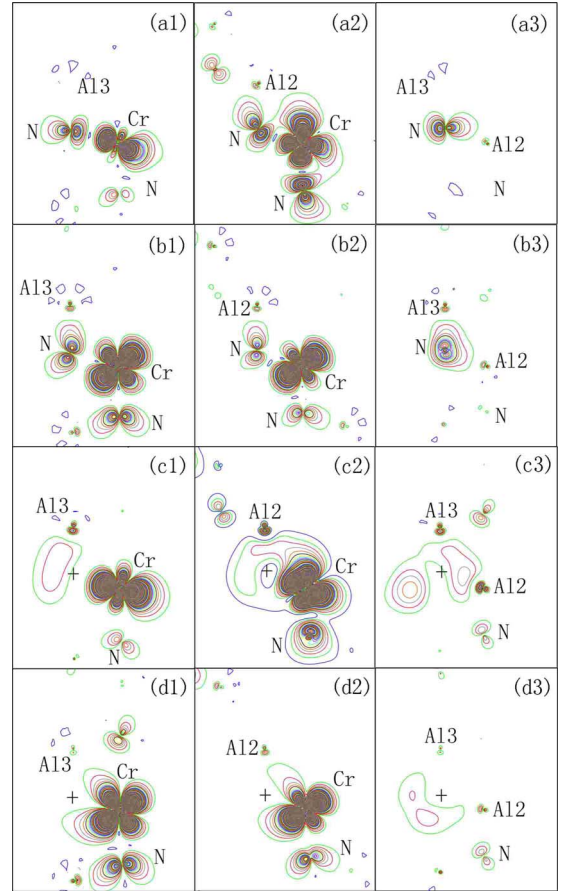


FIG. 5. (Color online) Electron-density distributions of the parts I (a1, a2, and a3) and II (b1, b2, and b3) of $\text{CrAl}_{35}\text{N}_{36}$ defined in panel (b) of Fig. 3 and those of the parts I (c1, c2, and c3) and II (d1, d2, and d3) of $\text{CrAl}_{35}\text{N}_{35}$ defined in panel (c) of Fig. 3, where the three planes are the same as those in Fig. 4. It should be pointed out that the part I of $\text{CrAl}_{35}\text{N}_{35}$ consists of two electrons, but that of the other consists of one electron only. The outmost (green or light gray) line represents $0.001e/\text{a.u.}^3$. The density contour increment is $0.001e/\text{a.u.}^3$.

around Cr. The remaining charge is around the nearest N sites. Therefore, we can conclude that Cr electronic configuration in a $\text{Cr}+V_{\text{N}}$ complex is d^4 , not d^3 . The extra electron comes from the N vacancy. Thus the valence state of the $\text{Cr}+V_{\text{N}}$ complex is $\text{Cr}^-+V_{\text{N}}^+$.

V. FERROMAGNETISM CORRELATED WITH N DEFECTS IN REAL SAMPLES

Because the minimal formation energy for forming a neutral N vacancy in AlN is -0.23 eV, a small concentration of N vacancies can be formed spontaneously in AlN under poor N condition. An N vacancy contributes μ_B to the moment, but our calculations show that spin interaction between N-vacancy spins is estimated to be zero within computational error. Hence N vacancies alone cannot form ferromagnetism. Because the minimal formation energy for forming a substitutional Cr in AlN is 0.04 eV, dilute Cr doping alone is easy to be realized in AlN at room temperature under N-rich

condition. High concentrations of Cr atoms have been doped into AlN,^{16,17,24,29,30} although the Cr formation energy may be larger when Cr-Cr interaction cannot be neglected. This implies that there is no barrier of formation energy in the dilute doping limit. The Cr-doped AlN can be ferromagnetic through some mechanism based on hybridization between local Cr *d* states and extended N *p* states.^{26–28}

The minimal formation energy for forming a Cr+ V_N complex is 0.77 eV. As a result, the concentration of such complex is at most 2.3×10^{-6} per Al site when the synthesis temperature is at 600 K, becomes 10^{-3} at 1140 K, and reaches to 1% at 1700 K. Each of the Cr+ V_N complexes contributes $4\mu_B$ to the total moment. It should be pointed out that the maximal equilibrium concentration of such complexes at 1000 K is lower at least by two orders of magnitude than the Cr concentrations of MBE-grown samples [nominally (2–7)%]^{18,19,21,22} and other ones [nominally (3–5)%]^{16,17,24,29,30} of (Al,Cr)N diluted magnetic semiconductors. Thus the synthesis of real samples is not through growth of the Cr+ V_N complexes.

It is reasonable to suppose that there coexist N vacancies, Cr atoms, and Cr+ V_N complexes in real samples and the fractional concentrations are dependent on synthesis conditions.^{18,19} Because of N pressure fluctuation during synthesis, a substitutional Cr and an N vacancy can be formed easily in different regions. This implies that some N-vacancy domains and some Cr-doping domains can be formed simultaneously in separated different regions. The former is paramagnetic and the latter is ferromagnetic, but these domains are subjected to thermodynamical equilibrium of electrons in real samples. We present the schematic DOS and the corresponding Fermi levels of $\text{Al}_{36}\text{N}_{36}$, $\text{Al}_{36}\text{N}_{35}$ (including one N vacancy in the supercell), $\text{CrAl}_{35}\text{N}_{35}$ (including one Cr+ V_{N1} complex), $\text{CrAl}_{35}\text{N}_{36}$ (including one Cr substitutional at an Al site), and $\text{Cr}_2\text{Al}_{34}\text{N}_{36}$ (including Cr and Cr1 as defined in Fig. 1) in Figs. 6(a)–6(e). The Fermi level of $\text{CrAl}_{35}\text{N}_{36}$ is consistent with that of $\text{Cr}_2\text{Al}_{34}\text{N}_{36}$. Because the Fermi level of the N vacancy is substantially higher than that of the Cr atom, the electron of the N vacancy must transfer to the Cr site and this electron transfer results in pairs of V_N^+ and Cr^- . The Coulomb attraction between V_N^+ and Cr^- will make them tend to move together and form the neutral Cr+ V_N complex. Both of the Fermi levels of V_N^+ and the neutral Cr+ V_N complex are consistent with that of Cr atom. The electron of the N vacancy tends to be transferred to the Cr atom and the neutral Cr+ V_N complex.

The N vacancy is in favor of the ferromagnetism through forming the Cr+ V_N complex which contributes $4\mu_B$ to the moment and Cr+ $2V_N$ complex which contributes $5\mu_B$. On the other hand, the N vacancy can be harmful to the ferromagnetism through destroying the ferromagnetic spin coupling between two nearest substitutional Cr atoms. We can figure out what will happen in terms of the two characteristic synthesis temperatures T_{s1} and T_{s2} ($>T_{s1}$) for $\text{Cr}_x\text{Al}_{1-x}\text{N}_{1-y}$, where x is Cr concentration and y is N-vacancy concentration. We suppose that there is no second phase and hence set $y < 2x$ in the following.²⁰ When $T < T_{s1}$, neither N vacancy nor Cr atom can diffuse. A little of the N-vacancy electrons will transfer to Cr domains but further electron transferring will be blocked by the built-in electric field formed by the

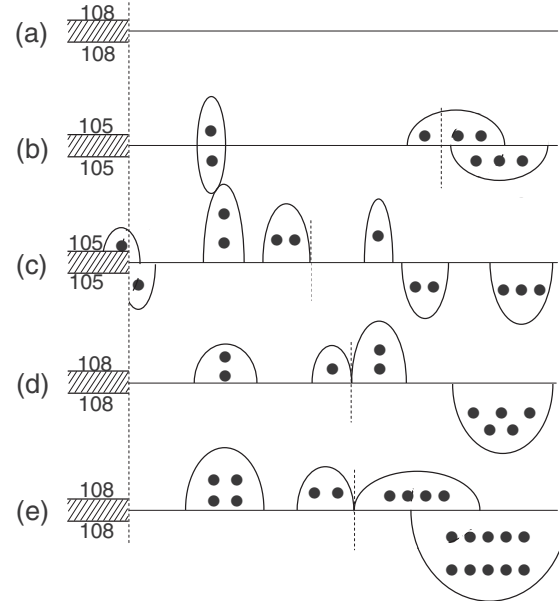


FIG. 6. Schematic DOS of (a) $\text{Al}_{36}\text{N}_{36}$, (b) $\text{Al}_{36}\text{N}_{35}$ (including one V_N), (c) $\text{CrAl}_{35}\text{N}_{35}$ (including one Cr+ V_{N1} complex), (d) $\text{CrAl}_{35}\text{N}_{36}$ (including one substitutional Cr atom), and (e) $\text{Cr}_2\text{Al}_{34}\text{N}_{36}$ (including two nearest substitutional Cr atoms). The two numbers for the shadow region denote the numbers of the majority-spin *p* valence bands and minority-spin ones. A solid dot means a filled electron in the bands.

transferred electrons. As a result, the main features of the domain patterns will remain. The Cr moments are coupled by thermally activated variable-range hopping of electrons,²⁴ and thus the N vacancy enhances the ferromagnetism.^{22,30} When $T_{s1} < T < T_{s2}$, N vacancy can diffuse but Cr atom cannot. All the N vacancies and their electrons will transfer to Cr domains, and many Cr+ V_N and Cr+ $2V_N$ complexes are formed. In this case, the coupling of moments is the same, but the conductivity becomes weaker because an additional barrier must be overcome for the electron to hop,²⁴ and thus the enhancement decreases with increasing y . When $T > T_{s2}$, both N vacancy and Cr atom can diffuse. Cr atoms tend to form clusters⁴⁵ (similar to Cr- and Mn-doped GaN)^{47–49} and the N vacancies tend to change the inter-Cr ferromagnetic coupling into antiferromagnetic coupling. In this temperature range, the N vacancy is harmful to the ferromagnetism. However, the N vacancy can be made to enhance the ferromagnetism by keeping the synthesis temperature below T_{s2} so that Cr clusters are unlikely. This is in good agreement with experimental observation that N vacancies enhance the ferromagnetism in samples made at low temperature.^{22,30}

VI. CONCLUSION

We have investigated nitrogen defects and their effects on the ferromagnetism of Cr-doped AlN with N vacancies using the full-potential density-functional-theory method and supercell approach. We investigate the structural and electronic properties of V_N , single Cr atom, Cr-Cr atom pairs, Cr- V_N pairs, and so on. In each case, the most stable structure is obtained by comparing different atomic configurations opti-

mized in terms of the total energy and the force on every atom and is then used to calculate the defect formation energy and study the electronic structures. Without N vacancy, two Cr atoms have the lowest energy when they stay at the nearest Al sites and their moments orient in parallel. An N vacancy and a Cr atom tend to form a stable complex of Cr^- and V_N^+ and the moment of $4\mu_B$ origins from the Cr d^4 electrons. Our calculated formation energies indicate that V_N regions can be formed spontaneously under N-poor condition or high enough concentrations of Cr atoms can be formed under N-rich condition, but only tiny concentrations of Cr + V_N complexes can be realized under usual experimental conditions. Both of the N vacancy and Cr atom create states in the semiconductor gap of AlN and the highest filled state of the N vacancy is higher than the filled Cr states. V_N enhances the ferromagnetism by giving one electron to Cr ion to add μ_B to the Cr moment but reduces the ferromagnetic exchange constants between the spins in the nearest Cr-Cr pairs.

The formation energy results imply that real Cr-doped samples with N vacancies are formed by forming Cr-doped regions and some separated V_N regions and through subsequent atomic relaxation during annealing. The V_N enhance-

ment of the ferromagnetism is in good agreement with experimental observation that low nitrogen pressure enhances the ferromagnetism of $\text{Al}_{1-x}\text{Cr}_x\text{N}_{1-y}$ when the synthesis temperature is low, so that Cr atoms cannot diffuse.^{22,30} On the other hand, too many N vacancies are harmful to the ferromagnetism when the synthesis temperature is high enough to make Cr atoms diffuse and tend to become clusters of secondary phases in which Cr-Cr spin interactions mainly are antiferromagnetic.^{21,22,29-31} However, we can make N vacancies enhance the ferromagnetism by keeping the synthesis temperature low enough to avoid Cr diffusion. All these first-principles results are useful to explore high-performance Cr-doped AlN DMS materials and to understand their high-temperature ferromagnetism.

ACKNOWLEDGMENTS

This work was supported by the Nature Science Foundation of China (Grants No. 10874232, No. 10774180, No. 90406010, and No. 60621091), by the Chinese Academy of Sciences (Grant No. KJCX2.YW.W09-5), and by the Chinese Department of Science and Technology (Grant No. 2005CB623602).

*Present address: Institute of Semiconductors, Chinese Academy of Sciences, 100083 Beijing, China.

†Corresponding author. bgliu@mail.iphy.ac.cn

- ¹S. A. Wolf, D. D. Awschalom, R. A. Buhrman, J. M. Daughton, S. von Molnar, M. L. Roukes, A. Y. Chtchelkanova, and D. M. Treger, *Science* **294**, 1488 (2001).
- ²T. Dietl, H. Ohno, F. Matsukura, J. Cibert, and D. Ferrand, *Science* **287**, 1019 (2000).
- ³S. Sanvito, P. Ordejon, and N. A. Hill, *Phys. Rev. B* **63**, 165206 (2001).
- ⁴T. Jungwirth, J. Sinova, J. Masek, J. Kucera, and A. H. MacDonald, *Rev. Mod. Phys.* **78**, 809 (2006), and references therein.
- ⁵J. M. D. Coey, *Curr. Opin. Solid State Mater. Sci.* **10**, 83 (2006).
- ⁶K. Ueda, H. Tabata, and T. Kawai, *Appl. Phys. Lett.* **79**, 988 (2001).
- ⁷S.-J. Han, T.-H. Jang, Y. B. Kim, B.-G. Park, J.-H. Park, and Y. H. Jeong, *Appl. Phys. Lett.* **83**, 920 (2003).
- ⁸M. H. F. Sluiter, Y. Kawazoe, P. Sharma, A. Inoue, A. R. Raju, C. Rout, and U. V. Waghmare, *Phys. Rev. Lett.* **94**, 187204 (2005).
- ⁹Y. Matsumoto, M. Murakami, T. Shono, T. Hasegawa, T. Fukumura, M. Kawasaki, P. Ahmet, T. Chikyow, S. Koshihara, and H. Koinuma, *Science* **291**, 854 (2001).
- ¹⁰S. R. Shinde, S. B. Ogale, S. Das Sarma, J. R. Simpson, H. D. Drew, S. E. Lofland, C. Lanci, J. P. Buban, N. D. Browning, V. N. Kulkarni, J. Higgins, R. P. Sharma, R. L. Greene, and T. Venkatesan, *Phys. Rev. B* **67**, 115211 (2003).
- ¹¹S. B. Ogale, R. J. Choudhary, J. P. Buban, S. E. Lofland, S. R. Shinde, S. N. Kale, V. N. Kulkarni, J. Higgins, C. Lanci, J. R. Simpson, N. D. Browning, S. Das Sarma, H. D. Drew, R. L. Greene, and T. Venkatesan, *Phys. Rev. Lett.* **91**, 077205 (2003).
- ¹²J. M. D. Coey, A. P. Douvalis, C. B. Fitzgerald, and M. Venkate-

san, *Appl. Phys. Lett.* **84**, 1332 (2004).

- ¹³J. Philip, A. Punnoose, B. I. Kim, K. M. Reddy, S. Layne, J. O. Holmes, B. Satpati, P. R. Leclair, T. S. Santos, and J. S. Moodera, *Nature Mater.* **5**, 298 (2006).
- ¹⁴J. M. D. Coey, M. Venkatesan, and C. B. Fitzgerald, *Nature Mater.* **4**, 173 (2005).
- ¹⁵S. Sonoda, S. Shimizu, T. Sasaki, Y. Yamamoto, and H. Hori, *J. Cryst. Growth* **237-239**, 1358 (2002).
- ¹⁶S. Y. Wu, H. X. Liu, L. Gu, R. K. Singh, L. Budd, M. van Schilfgaarde, M. R. McCartney, D. J. Smith, and N. Newman, *Appl. Phys. Lett.* **82**, 3047 (2003).
- ¹⁷D. Kumar, J. Antifakos, M. G. Blamire, and Z. H. Barber, *Appl. Phys. Lett.* **84**, 5004 (2004).
- ¹⁸H. X. Liu, S. Y. Wu, R. K. Singh, L. Gu, D. J. Smith, N. Newman, N. R. Dilley, L. Montes, and M. B. Simmonds, *Appl. Phys. Lett.* **85**, 4076 (2004).
- ¹⁹L. Gu, S. Y. Wu, H. X. Liu, R. K. Singh, N. Newman, and D. J. Smith, *J. Magn. Magn. Mater.* **290-291**, 1395 (2005).
- ²⁰R. M. Frazier, J. Stapleton, G. T. Thaler, C. R. Abernathy, S. J. Pearton, R. Rairigh, J. Kelly, A. F. Hebard, M. L. Nakarmi, K. B. Nam, J. Y. Lin, H. X. Jiang, J. M. Zavada, and R. G. Wilson, *J. Appl. Phys.* **94**, 1592 (2003).
- ²¹A. Y. Polyakov, N. B. Smirnov, A. V. Govorkov, R. M. Frazier, J. Y. Liefer, G. T. Thaler, C. R. Abernathy, S. J. Pearton, and J. M. Zavada, *Appl. Phys. Lett.* **85**, 4067 (2004).
- ²²R. M. Frazier, G. T. Thaler, J. P. Leifer, J. K. Hite, B. P. Gila, C. R. Abernathy, and S. J. Pearton, *Appl. Phys. Lett.* **86**, 052101 (2005).
- ²³A. Fara, F. Bernardini, and V. Fiorentini, *J. Appl. Phys.* **85**, 2001 (1999).
- ²⁴S. G. Yang, A. B. Pakhomov, S. T. Hung, and C. Y. Wong, *Appl. Phys. Lett.* **81**, 2418 (2002).

- ²⁵S. Y. Wu and N. Newman, *Appl. Phys. Lett.* **89**, 142105 (2006).
- ²⁶B. Sanyal, O. Bengone, and S. Mirbt, *Phys. Rev. B* **68**, 205210 (2003).
- ²⁷M. Wierzbowska, D. Sanchez-Portal, and S. Sanvito, *Phys. Rev. B* **70**, 235209 (2004).
- ²⁸L.-J. Shi and B.-G. Liu, *Phys. Rev. B* **76**, 115201 (2007).
- ²⁹J. Zhang, S. H. Liou, and D. J. Sellmyer, *J. Phys.: Condens. Matter* **17**, 3137 (2005).
- ³⁰J. Zhang, X. Z. Li, B. Xu, and D. J. Sellmyer, *Appl. Phys. Lett.* **86**, 212504 (2005).
- ³¹Y. Endo, T. Sato, A. Takita, Y. Kawamura, and M. Yamamoto, *IEEE Trans. Magn.* **41**, 2718 (2005).
- ³²A. J. Behan, A. Mokhtari, H. J. Blythe, D. Score, X.-H. Xu, J. R. Neal, A. M. Fox, and G. A. Gehring, *Phys. Rev. Lett.* **100**, 047206 (2008).
- ³³S. Yoshii, S. Sonoda, T. Yamamoto, T. Kashiwagi, M. Hagiwara, Y. Yamamoto, Y. Akasaka, K. Kindo, and H. Hori, *Europhys. Lett.* **78**, 37006 (2007).
- ³⁴P. Larson and S. Satpathy, *Phys. Rev. B* **76**, 245205 (2007).
- ³⁵P. Hohenberg and W. Kohn, *Phys. Rev.* **136**, B864 (1964); W. Kohn and L. J. Sham, *ibid.* **140**, A1133 (1965).
- ³⁶P. Blaha, K. Schwarz, P. Sorantin, and S. B. Trickey, *Comput. Phys. Commun.* **59**, 399 (1990).
- ³⁷J. P. Perdew, K. Burke, and M. Ernzerhof, *Phys. Rev. Lett.* **77**, 3865 (1996).
- ³⁸J. P. Perdew and Y. Wang, *Phys. Rev. B* **45**, 13244 (1992).
- ³⁹Ph. Mavropoulos, K. Sato, R. Zeller, P. H. Dederichs, V. Popescu, and H. Ebert, *Phys. Rev. B* **69**, 054424 (2004).
- ⁴⁰Q. Wang, A. K. Kandalam, Q. Sun, and P. Jena, *Phys. Rev. B* **73**, 115411 (2006).
- ⁴¹S. B. Zhang and J. E. Northrup, *Phys. Rev. Lett.* **67**, 2339 (1991).
- ⁴²S. B. Zhang and S.-H. Wei, *Phys. Rev. Lett.* **86**, 1789 (2001).
- ⁴³L. Bellard, C. Fauquet-Ben Ammar, J.-M. Themlin, and A. Cros, *J. Appl. Phys.* **83**, 7640 (1998).
- ⁴⁴T. Mattila and R. M. Nieminen, *Phys. Rev. B* **54**, 16676 (1996).
- ⁴⁵X. Y. Cui, D. Fernandez-Hevia, B. Delley, A. J. Freeman, and C. Stampfl, *J. Appl. Phys.* **101**, 103917 (2007).
- ⁴⁶M. G. Ganchenkova and R. M. Nieminen, *Phys. Rev. Lett.* **96**, 196402 (2006).
- ⁴⁷T. Hynninen, H. Raebiger, and J. von Boehm, *Phys. Rev. B* **75**, 125208 (2007).
- ⁴⁸X. Y. Cui, J. E. Medvedeva, B. Delley, A. J. Freeman, and C. Stampfl, *Phys. Rev. B* **75**, 155205 (2007).
- ⁴⁹X. Y. Cui, B. Delley, A. J. Freeman, and C. Stampfl, *Phys. Rev. B* **76**, 045201 (2007).